Air Traffic Conflict Models

Matt R. Jardin*
NASA Ames Research Center, Moffett Field, CA 94035

Semi-empirical random variable models of the expected number of air traffic conflicts as a function of air traffic density are derived. Model parameters are determined from analysis and simulation of real air traffic data. These models are applied to simulated air traffic scenarios to analyze conflict properties in various conflict resolution strategies. It is shown that under free routing conditions (i.e. aircraft do not necessarily fly along structured jet routes), the expected number of conflicts is well represented by a binomial random variable model. Using this model, it is further demonstrated how conflict resolution may cause a chain reaction, leading to an increased number of conflicts for all aircraft, and how the model may be used to predict the airspace capacity for a given conflict resolution strategy. In a separate study, it is shown that for an iterative horizontal-plane conflict resolution strategy, a random variable model with the geometric distribution closely matches empirical data. This model also predicts the aircraft density at which the airspace becomes saturated. It is shown how analysis of conflicts in the horizontal plane may be scaled and applied to the analysis of conflicts in 3-dimensional airspace.

I. Introduction

Current enroute air traffic control (ATC) operations are based on the use of structured jet routes. Aircraft are rarely permitted to operate along unstructured routes unless air traffic is sparse. The concept of Free Flight for ATC has evolved from the desire to create more efficient enroute air traffic operations.[1] The idea is that by allowing aircraft to determine and update their own unstructured flight routes while using automated onboard conflict detection and resolution algorithms, the ATC system will be more efficient. In low air traffic densities, as is the case with the current level of air traffic, some form of Free Flight is predicted to provide an efficiency benefit. At some increased level of air traffic density, the benefit of allowing aircraft to fly along unstructured routes can no longer be realized because the complexity of the airspace becomes a problem. It has been theorized that with increasing air traffic density, resolving conflicts will cause an increased number of conflicts. Simulation studies have been conducted in prior work and have shown that such a chain reaction may become significant at roughly three times the current air traffic density,[2] but physical explanations have not yet been offered.

In this paper, probabilistic models of air traffic conflict situations are derived and analyzed to gain physical insight into the relationship between increasing air traffic density and the expected number of conflicts between aircraft. The first section examines the expected number of conflicts under both a structured routing system and under a free routing system. It is shown that a binomial random variable model closely matches observations of the number of conflicts when conflict resolution is not applied. The effect of conflict resolution maneuvering on the expected number of conflicts is also examined. An analytical model is derived, and simulation results are used to verify the model. The second main section of this paper introduces a model of the expected number of conflicts when an iterative approach to conflict resolution is taken. This model is examined to show how it may be used to predict maximum airspace capacity.

*Aerospace Engineer, Code AFC, Automation Concepts Research Branch, MS 210-10. Senior Member AIAA.

II. Decentralized Conflict Resolution Models

In this section, probabilistic models of decentralized conflict processes are derived. The first model is of the expected number of conflicts when conflict resolution is not applied. The next model is of the expected number of conflicts with conflict resolution applied. A simulation is developed, and the results of the simulation are presented.

A. Modeling Conflicts Without Conflict Resolution

A study performed at the NASA Ames Research Center examined the properties of air-traffic conflicts for both structured routing and great-circle routing.[2] Flight plan data were taken from the Enhanced Traffic Management System (ETMS) for a 24-hr period in March 2000. The Future Air Traffic Management Concepts Evaluation Tool (FACET)[3] was used to simulate aircraft flying either along the filed flight plans or along great-circle routes between the scheduled origin and destination airports within Class A airspace (above FL180). At each 15 second integration time-step, the number of active conflicts in the airspace was recorded, as was the total number of aircraft in the airspace at that time.

These conflict data may be used to evaluate the aircraft density of the airspace environment. A high number of conflicts and a steep rate of growth of conflicts would suggest that the airspace was nearing saturation. Conversely, a low number of conflicts and a shallow growth rate would suggest that the airspace still had plenty of extra maneuvering volume remaining.

The plot of the number of instantaneous conflicts versus the number of aircraft flying shows that for both structured routing and great-circle routing, the number of conflicts is relatively low, and the growth rate is also low (figure 1). Without assuming any prior knowledge of aircraft paths, it is equally likely that one aircraft will be in conflict with any other aircraft. This suggests that the instantaneous number of conflicts, X, for any aircraft may be modeled as a binomial random variable such that the probability mass function is given by

$$P(X = x) = \binom{n}{x} p^x (1-p)^{n-x} \qquad \begin{cases} 0 \le p \le 1 \\ x = 0, 1, \ldots, n \end{cases} \tag{1}$$

where $n \equiv (N_{ss} - 1)$, N_{ss} is the steady-state number of aircraft flying (a measure of aircraft density for a given airspace area), p is the probability that any one aircraft will have a conflict with any one other aircraft at a given instant, and

$$\binom{n}{x} \Rightarrow n \text{ choose } x \Rightarrow \frac{n!}{x!(n-x)!} \tag{2}$$

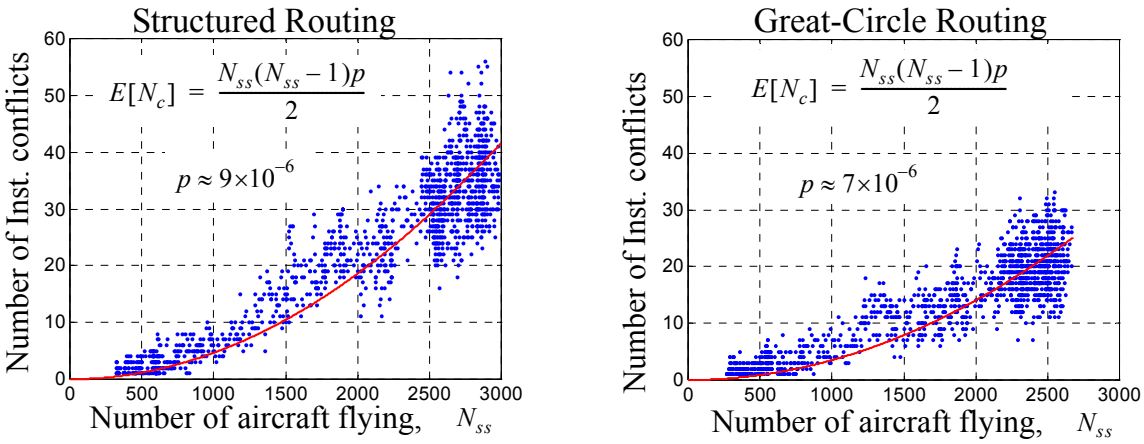

Fig. 1. Conflict counts for structured and great-circle routes.

With this model, the expected number of instantaneous conflicts for a single aircraft in a field of N_{ss} aircraft is given by

$$E[X_N] = (N_{ss} - 1)p \tag{3}$$

and the expected sum total number of instantaneous conflicts (divided in half so that conflicts are not counted twice) is given by

$$C_{INST} \equiv \sum_{i=1}^{N_{ss}} \frac{E[X]}{2} = \frac{N_{ss}(N_{ss} - 1)p}{2} \tag{4}$$

By choosing the aircraft-to-aircraft conflict probability, p, to fit the data in a least square error sense, the probabilities and expected values may be estimated for structured or great-circle routing. A table of results is presented based on the data shown in figure 1 (Table 1).

Table 1: Conflict statistics from binomial random variable model.

Statistic	Description	Flight plan	Great circle
p	Probability of aircraft i conflicting with any other aircraft j at a given instant in time	9×10^{-6}	7×10^{-6}
$E[X_{3000}]$	Expected number of conflicts per aircraft in Class A airspace with 3,000 aircraft at any given instant in time	0.027	0.021
$\sum_{i=1}^{3000} \frac{E[X]}{2}$	Expected sum total number of conflicts in Class A airspace with 3,000 aircraft at any given instant in time	40.5	31.5

These probabilities and expected numbers of conflicts are relatively low. In a field of 3,000 aircraft in Class A airspace above the continental United States, only about 2% of the aircraft would be expected to be involved in a conflict alert at any instant in time if no air traffic control action were taken. Conflict probabilities are lower for great-circle routing than for flight plan routing presumably because aircraft are able to utilize a greater amount of airspace.

The model in equation (4) may be extended to estimate the total number of expected conflicts, C_{NR}, for all aircraft in a given airspace area over a given interval of time when conflict resolution is not applied. In this case, p represents the probability that an aircraft, i, would experience a conflict alert with any other aircraft, j, during the analysis interval of time T. This probability may be decomposed into parts which are dependent upon airspace parameters and those which aren't.

Considering an airspace of area A which is divided into $N_{\Delta A}$ elements of area ΔA, the probability that any two aircraft i and aircraft j will occupy the same area element, ΔA, at the same time is given by

$$p = \left(\frac{\Delta A}{A}\right)^2 \tag{5}$$

Summing over all area elements leads to

$$p = N_{\Delta A}\left(\frac{\Delta A}{A}\right)^2 = \frac{\Delta A}{A} \tag{6}$$

The area of an element may be written in terms of the average area swept out by an aircraft as follows

$$\Delta A = p_t(D_{sep} \cdot V \cdot T) \tag{7}$$

where D_{sep} is the minimum separation distance between aircraft, V is the average aircraft speed, T is the time interval over which conflicts are counted, and p_t is a parameter which may be adjusted to match empirical data. Combining equations (6) and (7) leads to the following expression for the probability of conflict between any two aircraft

$$p = p_t\left(\frac{D_{sep} \cdot V \cdot T}{A}\right) \tag{8}$$

Writing p in this form separates out the dependency on airspace parameters so that the effects of changes in these parameters may more easily be discerned.

Equation (4) may be written in terms of airspace density, ρ_{AC}, by noting that

$$N_{ss} = \rho_{AC} \cdot A \tag{9}$$

Substituting equations (8) and (9) into equation (4) leads to the following expression for C_{NR}, the total number of conflicts if no resolution is applied

$$C_{NR} = p_t\left(\frac{D_{sep} \cdot V \cdot T \cdot A}{2}\right)\rho_{AC}(\rho_{AC} - 1/A) \tag{10}$$

B. Modeling Conflicts with Conflict Resolution: Conflict Chain Reactions

A conflict alert is defined as a condition in which two aircraft are predicted to be closer together than a specified minimum separation distance within a specified look-ahead distance (or time). Resolving aircraft conflicts using decentralized techniques may result in a chain reaction which increases the number of conflict alerts. If the increase in the number of conflicts is pronounced, the conflict resolution algorithms leading to the increase may be unstable. A study of this phenomenon was presented in Ref. 4.

The increase in conflicts due to conflict resolution was quantified in Ref. 4 by the "domino effect parameter (DEP)", defined as

$$DEP \equiv \left(\frac{C_{WR}}{C_{NR}} - 1\right) \tag{11}$$

where C_{NR} is the number of conflict alerts with no conflict resolution, and C_{WR} is the number of conflict alerts with conflict resolution applied.

A physical model is proposed in this section to explain conflict resolution chain reactions. The system considered is similar to that in Ref. 4. Aircraft are randomly generated at the same altitude in a 100 nmi radius airspace and are flying at the same ground speed. After conflicts are resolved, the aircraft are directed back to their originally planned exit point. Details of the conflict resolution are given later in the simulation results section of this paper.

The hypothesis is that for a given aircraft density in such a system, the rate of occurrence of conflict alerts (number of conflict alerts per unit time or distance) is constant whether or not aircraft perform conflict resolution maneuvers. This hypothesis is derived from the idea that there should be no preferred direction in such a system. It should be equally likely for any aircraft flying in any direction to experience a conflict. Just because an aircraft maneuvers does not change this fact. What does change is the total distance of flight in the test airspace, and the amount of airspace searched for conflicts. If the rate of conflicts is constant, but the total distance flown and searched for conflicts by all aircraft increases due to conflict resolution maneuvering, then one would expect the overall number of conflicts to increase. As aircraft density increases, and more conflict resolution maneuvers are required, the additional distance flown would also increase.

The expected number of conflicts, C_i, for aircraft i is expressed as

$$C_i = \bar{L} \cdot r_c \tag{12}$$

where $\bar{L}$ is the average path distance and r_c is the average rate of conflicts per unit distance.

The path distance is now modeled to increase in proportion to the number of conflicts so that equation (12) becomes

$$C_i = (L + k \cdot C_i)r_c \tag{13}$$

where L is the average nominal path distance of the aircraft in the simulation airspace without conflict resolution applied, k is a constant model parameter which includes both the average amount of extra path distance flown due to conflict resolution, and the effective extra path distance searched for conflicts per conflict resolution. As shown in figure 2, the effective amount of airspace searched for conflicts depends upon the conflict look-ahead distance and the length of the resolution portion of the trajectory.

Solving equation (13) for C_i leads to

$$C_i = \frac{L \cdot r_c}{1 - k \cdot r_c} \tag{14}$$

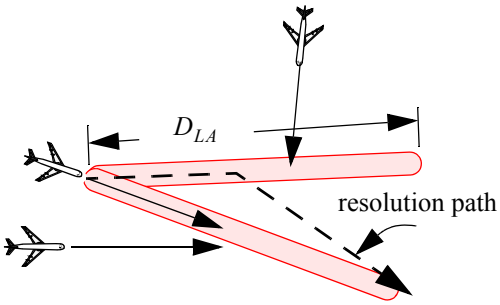

Fig. 2. Conflict resolution maneuvers cause additional airspace to be searched for conflicts.

Summing over N_{AC} aircraft, where N_{AC} is the total number of aircraft flying through the airspace (not the same as N_{ss}), leads to the following expression for the total number of conflicts with conflict resolution applied

$$C_{WR} = \frac{N_{AC} \cdot L \cdot r_c}{1 - k \cdot r_c} \tag{15}$$

The total number of conflict alerts without conflict resolution applied was given in equation (10). By the original hypothesis, the conflict rate should be the same for both the with-resolution and no-resolution cases. Using the no-resolution expression, the conflict rate may be written as the total number of no-resolution conflict alerts divided by the total path distance

$$r_c = \frac{C_{NR}}{N_{AC} \cdot L} \tag{16}$$

In order to maintain a given average airspace density over a given area and time, the number of aircraft must be

$$N_{AC} = \rho_{AC} \cdot A \cdot T \cdot (V/L) \tag{17}$$

Substituting equations (10), (15), (16), and (17) into equation (11) leads to the following relation for the domino effect parameter

$$DEP = \frac{(\rho_{AC} - 1/A)}{\rho_{max} - (\rho_{AC} - 1/A)} \tag{18}$$

where ρ_{max} is defined as

$$\rho_{max} \equiv \frac{2}{k \cdot p_t \cdot D_{sep}} \tag{19}$$

This parameter may either be chosen for analysis purposes, or determined empirically by adjusting its value until equation (18) best fits empirical data.

For values of ρ_{AC} much greater than $1/A$, an approximate version of equation (18) is given by

$$DEP \approx \frac{\rho_{AC}}{\rho_{max} - \rho_{AC}} \qquad \left| \rho_{AC} \gg (1/A) \right. \tag{20}$$

Note that ρ_{max} may be considered as a measure of the airspace capacity for the given conflict resolution scheme. The model of either equation (18) or (20) predicts that the chain reaction of conflicts will become infinite when ρ_{AC} approaches ρ_{max}, which makes intuitive sense since there is a finite amount of airspace. This leads to a practical and realistic means of computing the airspace capacity for a free-flight type of system with decentralized conflict resolution.

C. Decentralized Conflict Resolution Simulation Results

Monte Carlo simulations of randomly generated traffic have been run to generate data to validate the conflict model derived in this paper. Three different cases have been run for different values of separation distance, D_{sep} and conflict look-ahead distance, D_{LA}, to examine their effects upon conflict resolution. Each case was run with no-resolution and with-resolution at multiple values of N_{ss}, and multiple simulations were run for each value of N_{ss} in order to achieve some statistical variability. The pseudo-random-number generator from MATLAB was used to generate repeatable random cases so that the same traffic was run through both the no-resolution and with-resolution cases. The cases and values of N_{ss} used are given below in Table 2. The remaining parameters were common to all three cases and are given below in Table 3.

Table 2: Definitions of Simulation Cases

Case	D_{sep} (nmi)	D_{LA} (nmi)	$\{N_{ss}\} \times$ # of sims
1	5	66.7	$\{5, 10, \ldots, 35\} \times 15$ $\{40, 45, 50, 60, 80\} \times 3$
2	2.5	66.7	$\{5, 10, \ldots, 50, 60, 80, 85\} \times 3$
3	5	16.7	$\{5, 10, \ldots, 50, 60, 80, 85\} \times 3$

Table 3: Simulation Parameters

Parameter	Value(s)	Notes
R	100 nmi	Circular simulation area of radius R
$\bar{V}$	500 kn	All aircraft traveling at the same speed, $\bar{V}$
$\bar{L}$	$(4/\pi)R$	Average path-distance for uniformly random generated traffic across a circular area of radius R.
T	65.3 min	Simulation time duration. Note that simulation is also initialized for a duration of $\bar{L}/\bar{V}$ prior to starting data collection in order to populate the airspace
ΔT	2 seconds	Simulation time-step size
r_{AC}	$N_{ss}(\bar{V}/\bar{L})$	Rate of introduction of aircraft into simulation airspace to achieve N_{ss} steady-state aircraft

The details of how conflict resolution is performed, and how conflicts are counted are as follows:

- Conflict resolution maneuvers are computed according to the geometric conflict resolution algorithm in Ref. 5. Conflict resolution is non-cooperative such that only one aircraft involved in each conflict will maneuver. Of the multiple potential resolution solutions, the one which produces the greatest relative velocity is chosen in an effort to minimize the time to the turn-back point, where the aircraft may turn back to its original destination. The aircraft with the longest distance-to-go is the one to make the resolution maneuver.
- Aircraft which are generated with very short nominal paths are discarded, with new random paths being generated until nominal path distances are greater than 10% of the circle radius.

- Aircraft which start with pop-up conflicts with line-of-sight distance less than D_{sep} are allowed to continue, with a conflict being counted for the pop-up conflict.
- At each time-step, the turn-back path to the destination point is checked. Once it is clear, the aircraft turns back.
- If the turn-back path results in a conflict with a different aircraft than the one which caused the original conflict, then the turn-back path is taken, but the aircraft resolves the new turn-back conflict.
- Conflicts between any two particular aircraft are only counted once. This may miss some repeat conflicts that may occur after multiple resolution maneuvers, but eliminates the over-counting of conflicts when resolution maneuvers chatter.
- Conflict look-ahead is extended outside the circle so that conflicts which are projected to occur outside the circle are counted, and resolution maneuvers made. However, the rate of conflicts outside the circle will diminish with distance away from the circle since the aircraft density falls off quickly. Ideally, look-ahead distance should be small compared with the circle radius.
- Aircraft which maneuver to avoid conflicts and pass outside the circle are dropped from the simulation at the point where they exit the circle. This is a mechanism by which the airspace capacity limit manifests itself as aircraft are bounced outside of the simulation airspace.

A plot of the recorded trajectories is shown (figure 3) for a 65 minute simulation with a minimum separation distance of 5 nmi and an average of five aircraft within the 100 nmi circle in steady-state. In color reproductions of this paper, the conflict resolution segments are highlighted in red. This particular simulation had two aircraft which experienced multiple chain-reaction conflicts.

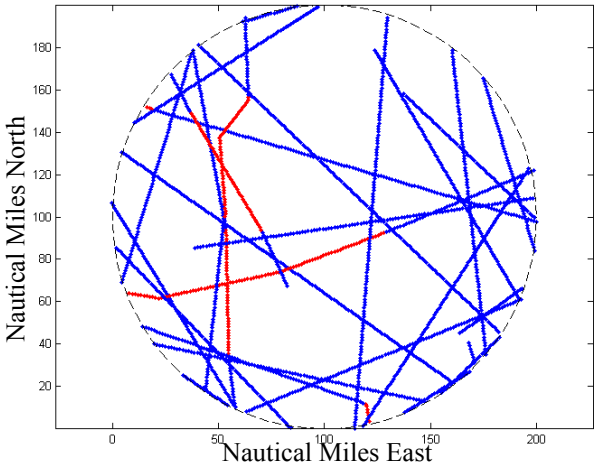

Fig. 3. Recorded trajectories for a 65 minute simulation with $N_{ss} = 5$, and $D_{sep} = 5$ nmi.

The results of the Monte Carlo simulation runs for the three different cases have been plotted together for comparison with one another (figure 4). The nominal case, with $D_{sep} = 5$ nmi and $D_{LA} = 66.7$ nmi, shows a clear trend along the curve predicted by equation (18) until the aircraft density exceeds 14 aircraft per 10^4 square nmi. As predicted by the model, an aircraft density is reached at which the airspace begins to become saturated. Since the simulation is of a finite airspace area, aircraft begin to be bounced outside of the airspace boundary due to conflicts as the airspace density limit is approached. Once these aircraft leave the simulation airspace, their conflicts are no longer counted, and this is why the empirical curve departs from the theoretical curve. The data points prior to the density limit being reached are used to determine the value of ρ_{max} which causes equation (18) to best-fit the empirical data in a least-square error sense.

Reducing the separation distance by a factor of 2, from 5 nmi to 2.5 nmi, increased the value of ρ_{max} by a factor of 2. Again, the departure of the simulation results from the model occurred when the aircraft density exceeded a critical threshold. For the parameters used in the simulation, the parameter k is dominated by the conflict look-ahead distance so that changes in the look-ahead distance should cause inversely proportional changes in ρ_{max}. A factor of 4 reduction in the conflict look-ahead distance from 8 minutes (equivalently 66.7 nmi at $V = 500$ kn) to 2 minutes (16.7 nmi) did result in approximately a factor of 4 increase in ρ_{max} as shown in figure 4.

D. Discussion of Decentralized Conflict Resolution Results

The derived conflict model clearly shows that reductions in either separation distance or look-ahead distance will increase the airspace capacity by a proportional amount. This suggests a method for considering global airspace efficiency when deciding how to perform decentralized conflict resolution.

Prior research considered the efficiency of conflict resolution maneuvering with trajectory prediction uncertainty.[6] It was shown that the expected extra distance flown could be minimized by resolving conflicts at an optimum conflict time horizon. As airspace density increases, the cascading effect of resolving conflicts too early (by having too large of a look-ahead time) incurs a large global penalty in efficiency. When global efficiency is considered, the optimum

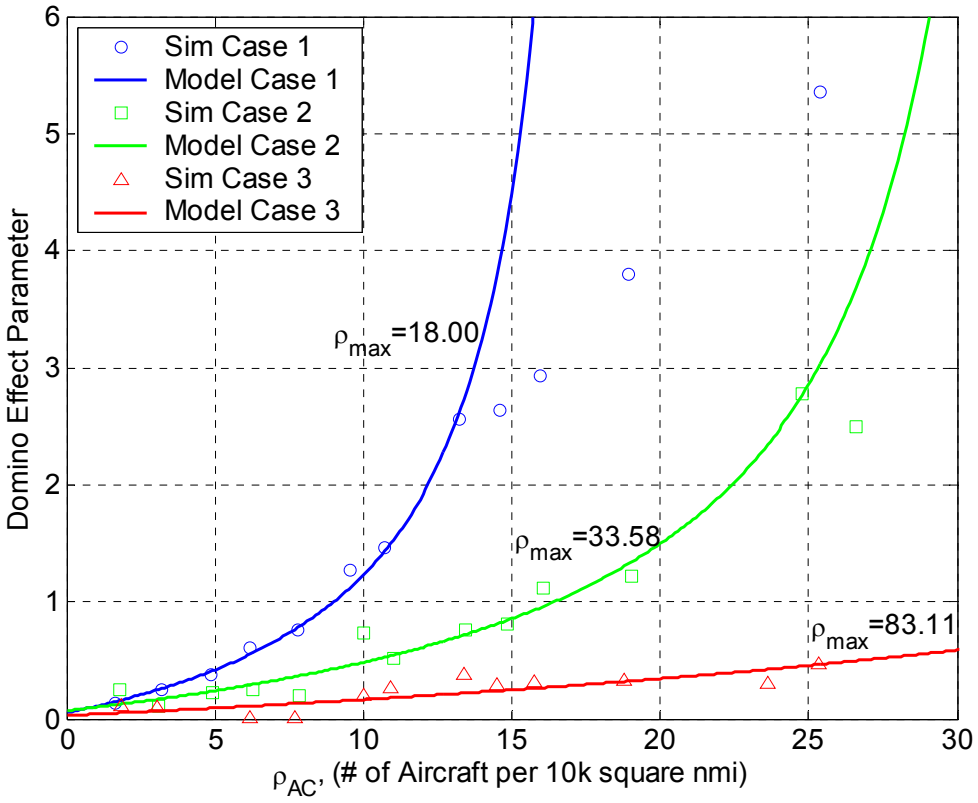

Fig. 4. Simulation data and models of conflict resolution chain reactions

time-horizon for performing conflict resolution will generally be different than if only individual aircraft efficiency were considered. This would be an interesting topic for future research.

III. Centralized Conflict Resolution Model: Sequential Conflict Resolution

In this section, a model is derived for a particular type of centralized conflict resolution based on sequentially resolving conflicts. The model is derived, followed by the presentation of simulation results.

A. Sequential Conflict Resolution Model

Sequential conflict resolution means that a conflict free trajectory is determined for each aircraft sequentially, while holding previously planned trajectories fixed. In this paper, an optimal wind routing algorithm called Neighboring Optimal Wind Routing (NOWR) is used to generate trajectories to demonstrate the sequential procedure,[7,8,9] but other route computation algorithms might also be used.

A high-level flowchart for the sequential conflict resolution algorithm is illustrated in figure 5. The algorithm places all scheduled aircraft into an ordered list called the Active Aircraft List (AAL), which includes all in-flight aircraft and aircraft scheduled to depart within a specified look-ahead time window. The optimal horizontal route for the first aircraft on the AAL is computed and checked for conflicts. Note that there will be no conflicts with other aircraft for the first aircraft in the AAL, but conflicts with regions of bad weather or with special-use airspace may occur. If any conflicts are found, the trajectory is iteratively modified until a conflict-free trajectory results. The algorithm proceeds through all aircraft on the AAL until all have optimal conflict-free trajectories. At this point, the trajectories may be issued to the aircraft as flight plan clearances, and the optimization procedure may be restarted as often as required.

The hypothesis is that for a sequential conflict-resolution strategy, it is equally likely at each iteration that another conflict may be encountered (fig. 6). This may be described as a *memoryless property*, and suggests the use of the geometric random variable (GRV) for the conflict iteration model, because the GRV is the only discrete random variable with the memoryless property.

If R_i is modeled as a GRV representing the number of iterations required to resolve all conflicts for the ith aircraft, where each resolution iteration is considered to be an independent Bernoulli trial with probability P_i of being conflict-free, then the probability mass function (pmf) for R_i is given by

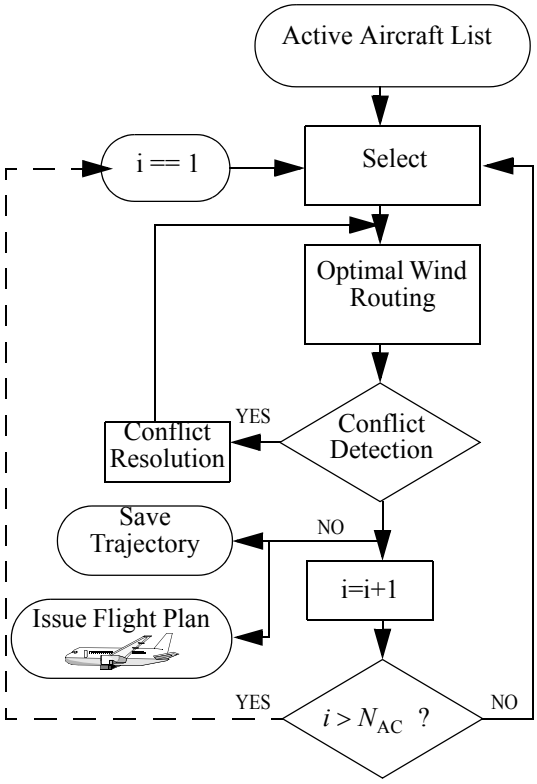

Fig. 5. Sequential route optimization flowchart.

$$p_{ik} = P_i(1-P_i)^{(k-1)} \begin{cases} i = 1, 2, \ldots, N \\ k = 1, 2, \ldots \end{cases} \tag{21}$$

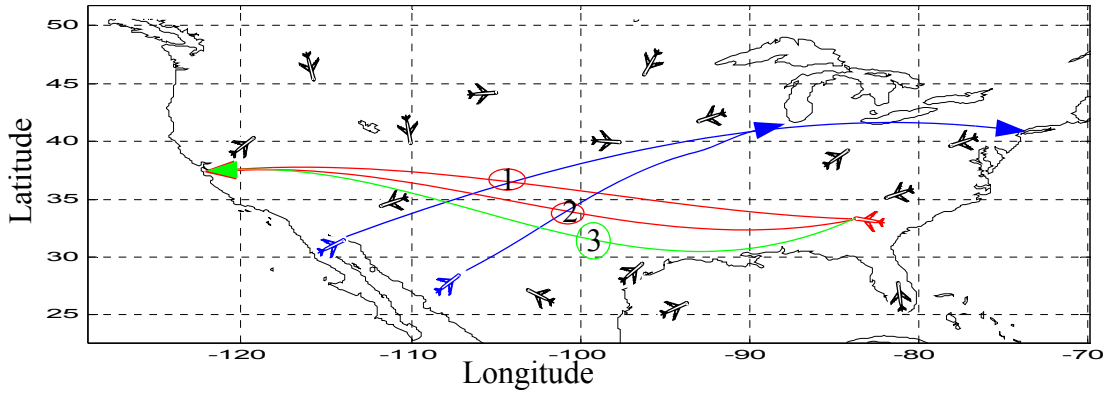

Fig. 6. Conflict probability is hypothesized to be memoryless.

where p_{ik} is the probability of resolving a conflict in k iterations for the i th aircraft. Typical values of P_i are close to unity so that the probability of finding a conflict-free solution during the first iteration is high, and the probability that a conflict-free trajectory will not be found until a later iteration decreases rapidly.

The expected value of the GRV, R_i, is

$$E[R_i] = \frac{1}{P_i} \tag{22}$$

As an extension to the standard GRV model, P_i is modeled as a function of the aircraft number. The reason for doing so is that the probability that a particular trajectory will be conflict-free decreases as the number of aircraft increases. The first aircraft will have a conflict-free trajectory with probability 1, while later aircraft will have increasing conflict probabilities. A linear form for P_i is chosen as

$$P_i = \frac{(C_0 + 1)}{C_1} - \frac{1}{C_1} i \tag{23}$$

where C_0 and C_1 are parameters that are to be determined to best fit observed data. The form for the coefficients of P_i was chosen to simplify the final results. The linear functional form was chosen because it is simple and leads to a good fit to empirical data. Other functional forms such as higher-order polynomials or exponential functions might also be used. The choice of functional form for P_i primarily affects model properties as the number of aircraft increases towards a limiting upper value.

Substituting equation (23) into equation (22) leads to

$$E[R_i] = \frac{C_1}{(C_0 + 1) - i} \tag{24}$$

To generate data to curve-fit equation (24), one would have to perform multiple simulations or experiments to generate many data points at each value of i so that the expected number of resolution iterations could be determined to some degree of statistical significance. A curve-fit of these expected values as a function of i could then be used to determine C_0 and C_1 in a least square error sense.

A better approach is to derive an expression for the sum of equation (24) over all aircraft. By doing so, only one simulation need be run while maintaining a running total of the number of conflict iterations. Each element of the sum is an independent measurement so that many independent measurements contribute to the sum as a function of the number of aircraft. A curve-fit of the summation function may then be used to obtain values for C_0 and C_1.

The summation of equation (24) leads to the following analytical expression:

$$Y_N \equiv \sum_{i=1}^{N} E[R_i] = \sum_{i=1}^{N} \frac{C_1}{(1 + C_0) - i} = C_1 \left(\Psi(C_0) - \Psi(C_0 - N) - \frac{N}{C_0(C_0 - N)} \right) \tag{25}$$

where $\Psi(x)$ is the *digamma* function, defined as

$$\Psi(x) \equiv \frac{\mathrm{d}}{\mathrm{d}x} \ln(\Gamma(x)) \tag{26}$$

and the *gamma* function, $\Gamma(x)$, is defined as

$$\Gamma(x) \equiv \int_0^{\infty} t^{(x-1)} e^{-t} dt \tag{27}$$

Although equation (25) is compact, it would be inconvenient to leave the expression in this form because the *digamma* function is not commonly used. In the region of interest for this problem, the *digamma* function is asymptotically close to the natural logarithm, $\ln(x)$. This leads to the following approximate form of equation (25):

$$Y_N \approx C_1 \ln\left(\frac{C_0}{C_0 - N} \right) - \frac{C_1 N}{C_0(C_0 - N)} \tag{28}$$

The second term in equation (28) turns out to be negligible for the types of problems being analyzed so that the total number of conflicts for N aircraft is well-approximated by

$$Y_N \approx C_1 \ln\left(\frac{C_0}{C_0 - N}\right) \tag{29}$$

By examining equation (23), one may determine some properties of the conflict-iteration model parameters. The first aircraft will only require one iteration (ignoring special-use airspace and weather cells for the moment), with probability 1, leading to the following relation:

$$P_1 = \frac{(C_0 + 1)}{C_1} - \frac{1}{C_1} = 1 \tag{30}$$

so one would expect

$$C_0 \approx C_1 \tag{31}$$

When curve-fitting empirical data, the fits obtained using two parameters are much better than single-parameter curve-fits because the data are not completely randomly distributed; for this reason, both parameters are retained. However, this analysis suggests that one might expect C_0 and C_1 to be numerically close.

Since aircraft typically cruise at near-constant altitude, a reasonable assumption is that the total number of conflicts across all flight levels is given by

$$Y_N\big|_{3D} = N_{FL} \cdot Y_N\big|_{2D} \tag{32}$$

where N_{FL} is the number of flight levels under consideration. The total number of aircraft, N_{3D} is given by

$$N\big|_{3D} = N_{FL} \cdot N\big|_{2D} \tag{33}$$

Under this assumption, the form of equation (29) is the same for the 3D problem as for the 2D problem with the constants being related in the following way

$$C_0\big|_{3D} \equiv N_{FL} \cdot C_0\big|_{2D} \tag{34}$$

$$C_1\big|_{3D} \equiv N_{FL} \cdot C_1\big|_{2D} \tag{35}$$

This assumption reduces the effort required to obtain results that apply to the full 3D problem. In the common flight altitudes of Class A airspace (FL180 through FL390), there are 17 distinct flight levels at which up to 5,000 aircraft may be found at any instant in time. Instead of running simulations of 5,000 or more aircraft to determine the model parameters of equation (29), one may run much simpler 2D simulations of about 300 aircraft ($5000/17$) at constant altitude. The values of C_0 and C_1 may be determined by curve-fitting the simulation data, and then equations (34) and (35) may be used to determine the equivalent values for the full Class A problem.

B. Sequential Conflict Resolution Simulation Results

A simulation was run in order to validate the derived conflict iteration model of equation (29). The data for the simulation were taken from the Enhanced Traffic Management System (ETMS) data feed for all aircraft in the continental United States domain at flight levels 330 and 350 on 10 August 2001. The origin, destination, and scheduled departure times were extracted from the data to generate a histogram of the number of flights during each hour along each city-pair route that appeared in the ETMS data. For the simulation, schedule data were generated randomly based on the ETMS distribution. In order to increase the number of flights in a realistic manner, 1.5 times the amount of actual traffic was generated in this way and used to drive the simulation according to the algorithm in figure 5.

For the particular simulation run shown in figure 7, aircraft included in the active aircraft list were those currently in the air, and those scheduled to depart within 30 minutes of the simulation start time. The plot shows the results of a single run through the active aircraft list. The wind data used for the simulation were from the Rapid Update Cycle, Version 2 (RUC2) from 2100 UTC, 2-hr forecast for the 225 mb pressure level. Note that 225 mb corresponds to approximately 36,000 ft.

The NOWR algorithm with iterative conflict resolution was used for route optimization. The conflict look-ahead time was set at 6.5 hours, and aircraft were considered to be in conflict when their relative distance fell below 10 nautical miles. Optimal wind routes were generated and checked for conflicts with previously planned aircraft trajectories. If a conflict was detected, the route was perturbed slightly and checked again until a conflict free route was found. The total number of conflict resolution iterations, Y_N, as a function of the number of aircraft, N, was recorded.

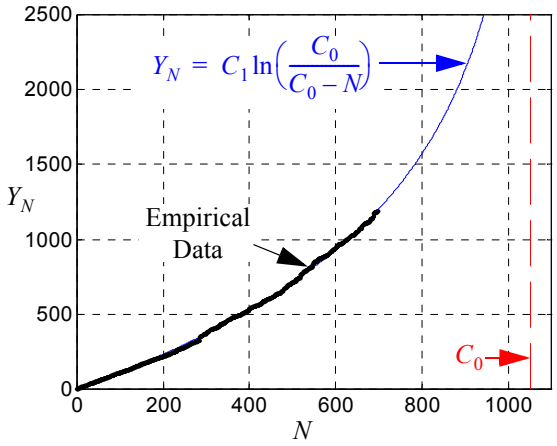

Fig. 7. Sequential Conflict Resolution Model

The shape of the Y_N vs. N curve from the model matches observations well. In this particular case, for the type of perturbation conflict resolution being used, the model predicts a maximum capacity of just over 1000 aircraft for a single flight level. This means that if this optimization and conflict resolution algorithm were in use, about 1000 aircraft could be accommodated before conflict-free routes could no longer be found. Note that the minimum separation distance in this example was 10 nautical miles, which is twice the current-day limit of 5 nautical miles. Also note that the route optimization algorithm being used generally does not search for conflict free paths which weave through traffic. Other optimization algorithms might be able to effectively use more airspace to increase the upper traffic bound. By comparison, the result of this example is between two and three times the maximum number of aircraft found at a single flight level at the peak time in today's constrained air traffic system (about 450). Simulations of other conflict resolution methods could be performed on the same data set in order to compare their performance with one another.

IV. Conclusion

Several semi-empirical models of aircraft conflicts have been presented in this paper. The expected number of conflicts for a given number of aircraft was shown to be well-modeled as a binomial random variable. This model was extended to show how different conflict resolution strategies might lead to a conflict chain reaction, and an increase in the total number of conflicts. The derived model predicts an upper limit on the number of aircraft that may operate within a given airspace. Some discussion was presented regarding how such a conflict model might be used to adjust conflict look-ahead times for distributed conflict resolution such that the total amount of extra flight distance due to conflict resolution is minimized over all aircraft.

For a sequential conflict resolution strategy, which is a type of centralized conflict resolution strategy, a semi-empirical model was developed to compute the expected number of conflict resolution iterations for a given number of aircraft. It was then shown how this model could be used to predict the capacity of a given airspace when using a particular sequential conflict resolution algorithm.

Acknowledgments

The author would like to thank Dr. Karl Bilimoria and Dr. Jimmy Krozel for providing information and data from their prior work on conflict resolution modeling. The author would also like to thank Dr. George Meyer and Dr. Larry Meyn for their thoughtful reviews of this material, and for their suggestions which have improved the final paper.

References

[1] "Free Flight Implementation," Final Report RTCA Task Force 3, RTCA, Inc., Washington, DC, Oct. 1995.

[2] Bilimoria, K. D., and Lee, H. Q., "Properties of Air Traffic Conflicts for Free and Structured Routing," AIAA2001-4051, AIAA Guidance, Navigation, and Control Conference, Montreal, Canada, Aug. 6-9, 2001.

[3] Bilimoria, K., Sridhar, B., et al., "FACET: Future ATM Concepts Evaluation Tool," *Air Traffic Control Quarterly*, Vol. 9, No. 1, 2001.

[4] Krozel, J., Peters, M., et al, "System Performance Characteristics of Centralized and Decentralized Air Traffic Separation Strategies," *Air Traffic Control Quarterly*, Vol. 9, No. 4, 2001.

[5] Bilimoria, K., "A Geometric Optimization Approach to Aircraft Conflict Resolution," AIAA 2000-4265, AIAA Guidance, Navigation, and Control Conference, Denver, Colorado, 14-17 August, 2000.

[6] Erzberger, H., Paielli, R., et al, "Conflict Detection and Resolution in the Presence of Prediction Error," 1st USA/Europe Air Traffic Management R&D Seminar, Saclay, France, 17-20 June, 1997.

[7] Jardin, M. R., Bryson, A. E. Jr., "Neighboring Optimal Aircraft Guidance in Winds," *Journal of Guidance, Control, and Dynamics*, Vol. 24, No. 4, Jul-Aug 2001, pp. 710-715.

[8] Jardin, M. R., "Toward Real-Time En Route Air Traffic Control Optimization," Ph.D. Dissertation, Stanford University Dept. of Aeronautics & Astronautics, April 2003.

[9] Jardin, M. R., "Neighboring Optimal Aircraft Guidance in a General Wind Environment," U.S. Patent 6,600,991, Jul. 29, 2003.

[10] Benjamin, S.G., J.M. Brown, K.J. Brundage, B.E. Schwartz, T.G. Smirnova, T.L. Smith, L.L. Morone, 1998: RUC-2 - The Rapid Update Cycle Version 2. NWS Technical Procedure Bulletin No. 448. NOAA/NWS, 18 pp. [National Weather Service, Office of Meteorology, 1325 East-West Highway, Silver Spring, MD 20910]